Supplementary Information (SI) for ChemComm.
This journal is © The Royal Society of Chemistry 2026

Supplementary Information

Ultrathin pillar-layered MOF membranes with narrow apertures toward ultrafast hydrogen purification

Zhiyi Li, Yihao Xiao, and Wanbin Li*

College of Environment and Climate, Jinan University, Guangzhou 511443, P.R. China

*Corresponding author email address: gandeylin@126.com (W.L.)

Methods

Materials and chemicals

Zinc acetate dihydrate ($Zn(CH_3COO)_2 \cdot 2H_2O$, 99%) and 1,2,4-triazole ($C_2H_3N_3$, ≥ 99%) were purchased from Aladdin. Zinc oxalate dihydrate ($ZnC_2O_4 \cdot 2H_2O$, ≥ 99%), sodium oxalate ($Na_2(C_2O_4)$, 99.5%), and 3-amino-1,2,4-triazole ($C_2H_4N_4$, 96%) were purchase from Macklin. Methanol (MeOH, ≥ 99.5%) was purchased from Guangdong Guanghua Sci-Tech Co. Polyethersulfone (PES) and polyacrylonitrile (PAN) ultrafiltration membranes with molecular weight cut-off of 100 kDa were purchased from Shanghai Hua Membrane Industry Co., Ltd. All the reagents were applied without any further purification. Deionized (DI) water was used in all experiments.

Synthesis of CALF-20 membrane

Zinc acetate dihydrate was dissolved in a mixed solvent containing water (16.0 mL) and MeOH (4.0 mL) by stirring to form a clear solution with zinc concentration of 12.5, 25, 37.5, 50, 75 mM, respectively. Sodium oxalate and 1,2,4-triazole were added into another same mixed solvent. Two solutions were separately added into left and right side of U-shaped device separated by using a PES membrane. Zinc/oxalate/1,2,4-triazole molar ratio was 2:1:4. Then, the interfacial growth was performed at 60 ^{o}C for 24 h. After reaction, the CALF-20 membrane was washed with DI water and MeOH for three times. The procedures for the CALF-20 membrane with PAN substrate were the same as those with PES.

Synthesis of CALF-20 powder

The CALF-20 powder was prepared by the precursor mixing method with the same precursor solutions under the same conditions as membrane preparation. Briefly, metal solution with zinc concentration of 37.5 mM and linker solution with oxalate concentration of 18.75 mM and 1,2,4-triazole concentration of 75 mM were mixed and heated at 60 ^{o}C for 24 h. After crystallization, the white powders were washed with DI water and MeOH for three times and collected by centrifugation. Ultimately, the powder was dried at 60 ^{o}C.

Besides, the CALF-20 powder was also synthesized by the solvothermal method.[1,2] Zinc oxalate dihydrate (43 mmol), 1,2,4-triazole (72.4 mmol), and MeOH (66 mL) were add into Teflon-lined stainless steel autoclave and thermally treated at 180 ^{o}C for 48 h. After reaction, the prepared powder was washed with MeOH for three times and collected by centrifugation. Ultimately, the powder was dried at 60 ^{o}C.

Synthesis of CALF-15 membrane

The CALF-15 membrane was prepared under the same conditions as for the CALF-20 membrane, except replacing 1,2,4-triazole by 3-amino-1,2,4-triazole.

Gas separation performance

Gas separation performance was evaluated by Wicke-Kallenbach technique. A membrane sample with an effective area of 2.0 cm^2 was sealed by O-rings in a permeation cell. The binary H_2/CO_2 gas mixture was injected into the feed side with a total flow rate of 200 mL min^{-1}. Ar was used as the sweep gas with flow rate of 150 mL min^{-1}. Gas components were

analyzed by using a gas chromatograph (GC-9280). Gas fractions and flow rates were controlled by using mass flow meters. The permeance (P) was calculated using Equation 1.

$$P = \frac{N}{\Delta P \times A} \tag{1}$$

N was molar flow rate of gas component; ΔP (Pa) was transmembrane pressure; and A (m^2) was effective membrane area.

Selectivity is calculated using Equation 2.

$$Selectivity = \frac{y_i/y_j}{x_i/x_j} \tag{2}$$

x_i and x_j represent fractions of components of i and j in feed gas, respectively; and y_i and y_j represent fractions of components i and j in permeate gas, respectively.

Characterizations

X-ray diffraction (XRD) patterns with 2θ range of 5-25 °were collected on D8 advance (Bruker Co., Germany). Cu $K\alpha$ radiation with a wavelength of 1.54056 Å was used for measurement. A field mission scanning electron microscope (FE-SEM, Ultra-55, Zeiss Co., Germany) was used to observe the membrane morphology. A Fourier transform infrared spectrometer (FTIR, Nicolet iS50, Thermo Fisher Scientific Inc., USA) and a x-ray photo-electron spectrometer (XPS, K-Alpha, Thermo Fisher Scientific Inc., USA) were employed to analyse the chemical structures. A physisorption analyser (Autosorb iQ Station 1, Quantachrome Co., USA) was used to collect the CO_2 adsorption isotherms at 273 and 298 K. Before measurement, the samples were outgassed at 130 ^oC under vacuum for 12 h.

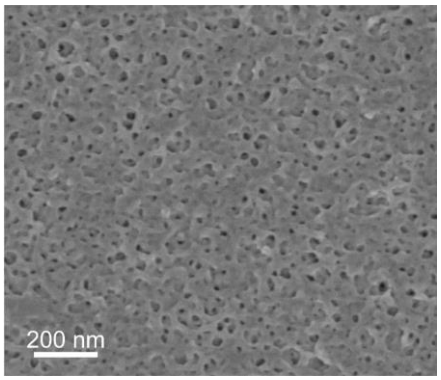

Fig. S1. Top-view SEM image of PES substrate.

Fig. S2. Digital photo of home-made U-shaped device for membrane fabrication.

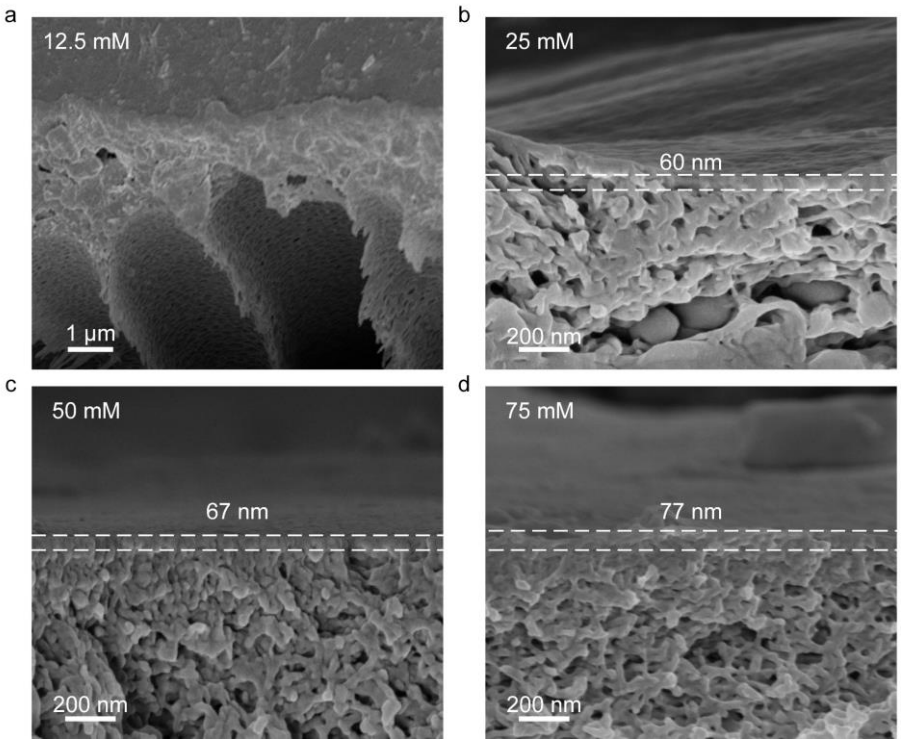

Fig. S3. Cross-sectional SEM images of CALF-20 prepared with zinc/oxolate/triazole ratio of 2:1:4 and different zinc concentrations of 12.5, 25, 50, and 75 mM.

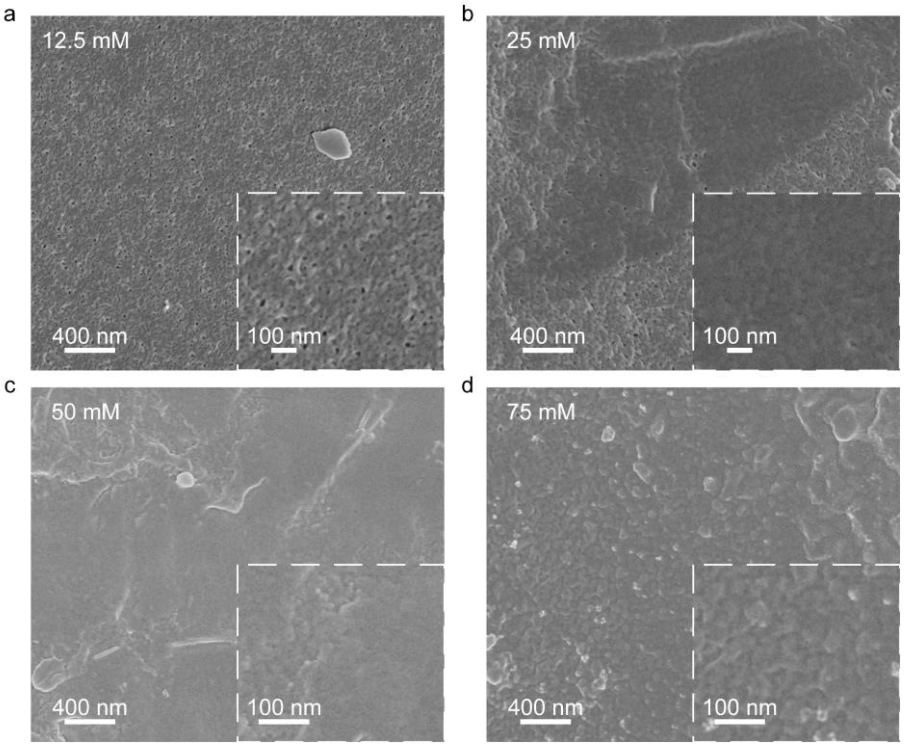

Fig. S4. Top-view SEM images of CALF-20 membranes prepared with zinc/oxolate/triazole ratio of 2:1:4 and different zinc concentrations of 12.5, 25, 50, and 75 mM.

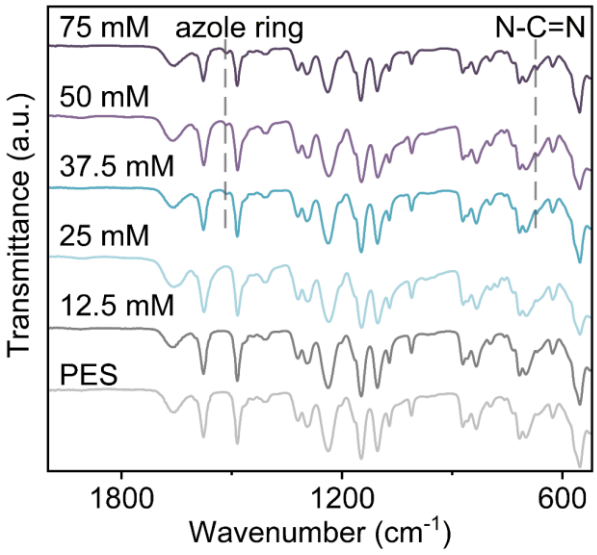

Fig. S5. FTIR spectra of PES and CALF-20 membranes.

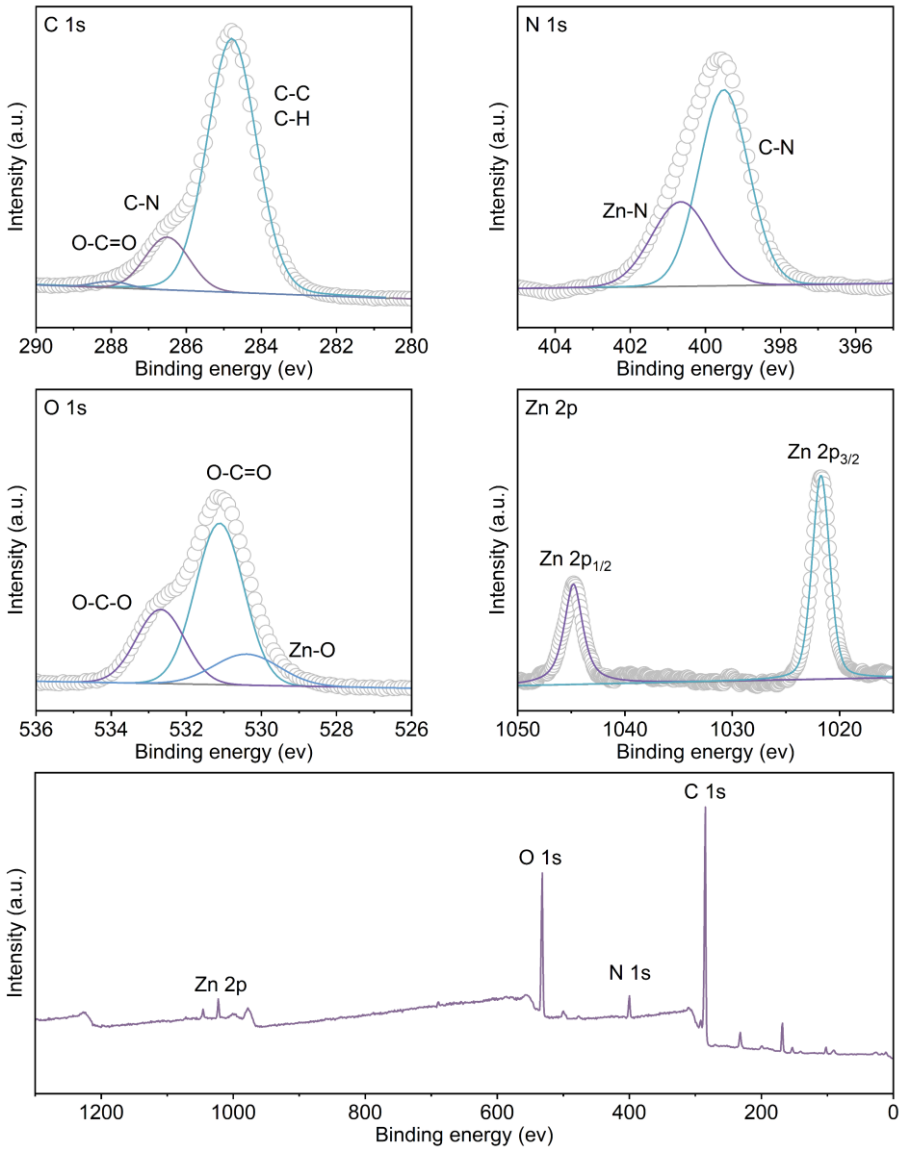

Fig. S6. XPS spectra of CALF-20 membrane.

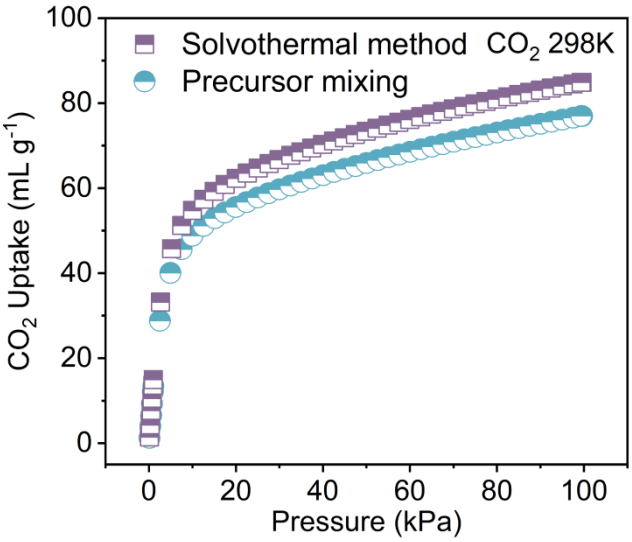

Fig. S7. CO_2 adsorption isotherms of CALF-20 synthesized by different methods at 298 K.

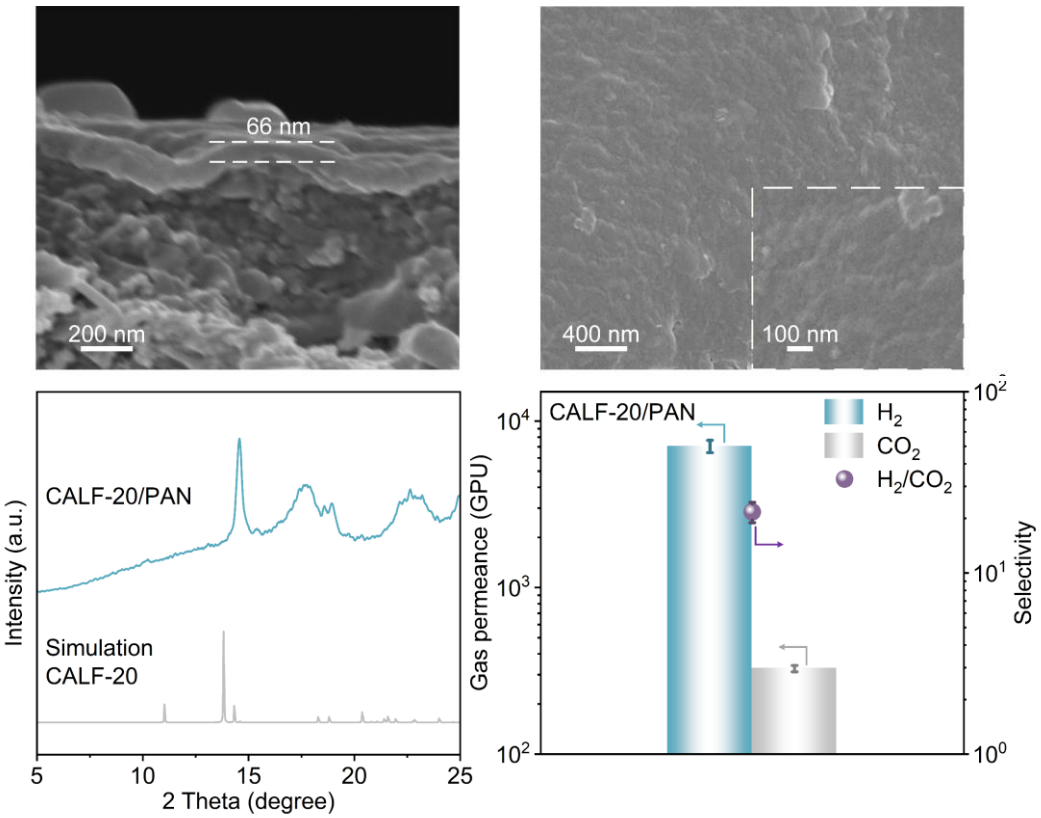

Fig. S8. SEM images, XRD patterns, and separation performance of CALF-20 membrane prepared on PAN substrate.

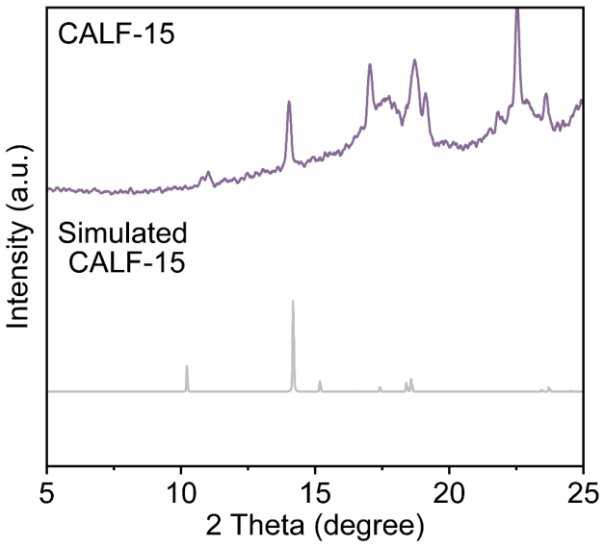

Fig. S9. XRD patterns of CALF-15 membrane and simulated CALF-15.

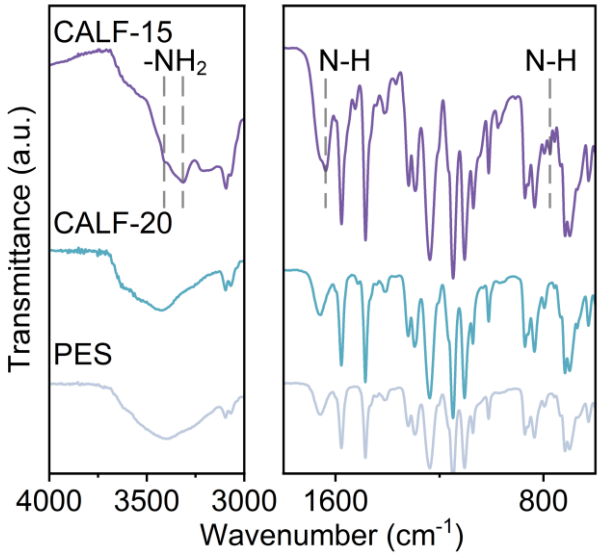

Fig. S10. FTIR spectra of PES, CALF-20, and CALF-15 membranes.

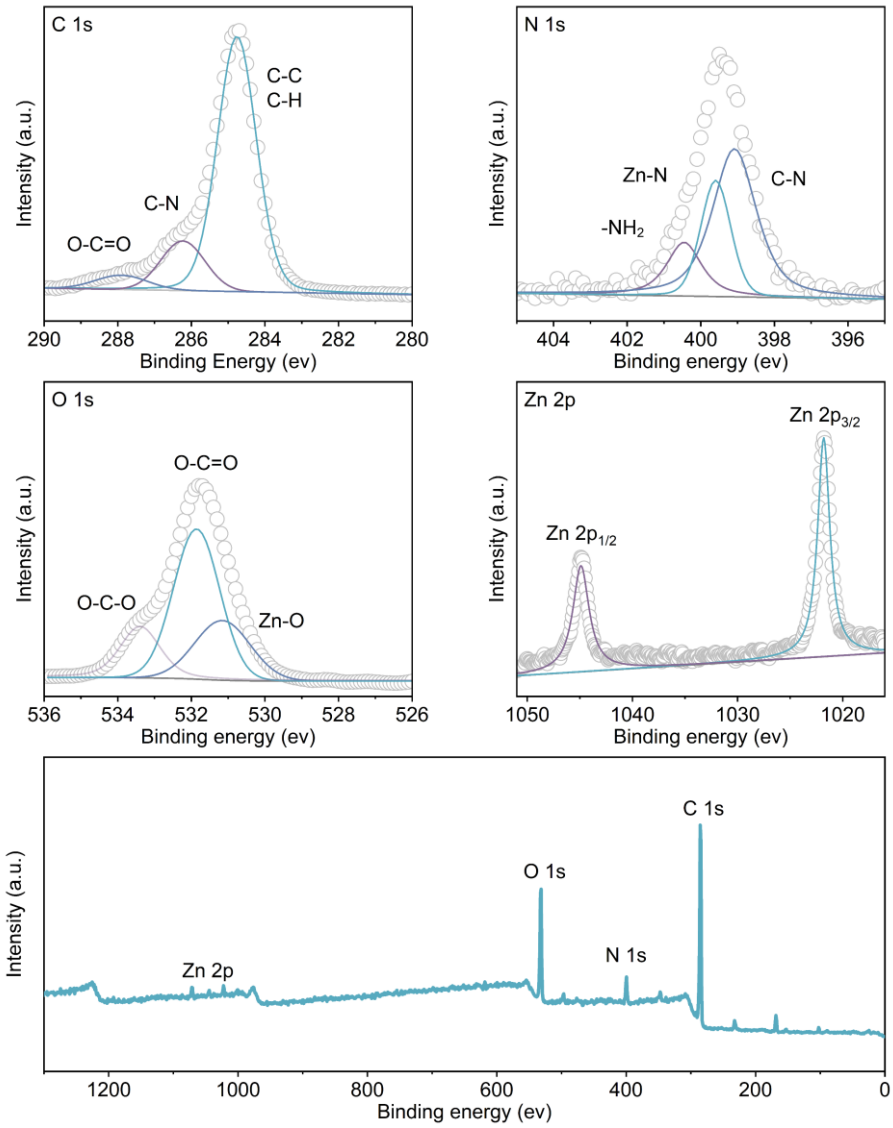

Fig. S11. XPS spectra of CALF-15 membrane.

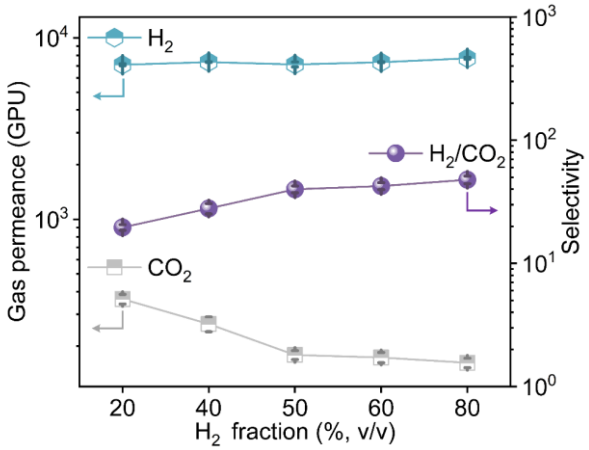

Fig. S12. Effect of feed gas composition on the permeance of CALF-15 membrane.

Table S1. Separation performance of polymer, MOF, and mixed-matrix membranes. Per: permeance, Sel: selectivity; T: temperature; PP: polypropylene; PAN: polyacrylonitrile; PVDF: poly(vinylidene fluoride); PBI: polybenzimidazole; PEI: polyethyleneimine; PBDI: poly(p-phenylene benzobisimidazole). BILP: Benzimidazole-linked polymers; and sPPSU: polyphenylsulfone.

Membranes	H_2 Per. (GPU)	H_2/CO_2 Sel.	Feed gas	T (^oC)	Ref
PBI	57.2	3.46	Single gas	20	3
PBI	65	17.6	Mixed gas	150	4
PBDI	241	23	Mixed gas	150	5
BILP-101x	30.1	31.6	Mixed gas	150	6
m-PBI	48.5	33.3	Mixed gas	180	7
PBI/sPPSU	16.7	9.7	Mixed gas	90	8
PMDA-MA PI	75.9	13	Mixed gas	300	9
PBI-Matrimid	38.67	6.85	Mixed gas	35	10
ZIF-7/α-A_2O_3	1425	9.59	Mixed gas	25	11
ZIF-7/PP	480	7.9	Mixed gas	35	12
ZIF-8/PAN	911.95	6.85	Mixed gas	20	13
ZIF-8/PVDF	5689.97	12.42	Mixed gas	RT	14
ZIF-95/α-A_2O_3	2392	32.2	Mixed gas	25	15
ZIF-9/α-A_2O_3	339	21.5	Mixed gas	25	16

ZIF-9/α-A_2O_3	554.4	23.8	Single gas	25	17
UiO-66/Matrimid/α-A_2O_3	1576.72	5.1	Mixed gas	25	18
NH_2-UIO-66/α-A_2O_3	1039.4	28.2	Mixed gas	20	19
KAUST-7/α-A_2O_3	657	17.7	Mixed gas	25	20
ZIF-67/PSS	167.165	9.3	Mixed gas	25	21
ZIF-8/PBI	20.3	35.6	Mixed gas	250	22
ZIF-7-NH_2/Pebax-1657	290	19	Mixed gas	RT	23
UiO-66/PEI	845	16.8	Mixed gas	35	24

References

1 J.-B. Lin, T. T. T. Nguyen, R. Vaidhyanathan, J. Burner, J. M. Taylor, H. Durekova, F. Akhtar, R. K. Mah, O. Ghaffari-Nik, S. Marx, N. Fylstra, S. S. Iremonger, K. W. Dawson, P. Sarkar, P. Hovington, A. Rajendran, T. K. Woo and G. K. H. Shimizu, *Science*, 2021, **374**, 1464–1469.

2 Y. Wei, F. Qi, Y. Li, X. Min, Q. Wang, J. Hu and T. Sun, *RSC Adv.*, 2022, **12**, 18224–18231.

3 S. C. Kumbharkar and K. Li, *J. Membr. Sci.*, 2012, **415**–**416**, 793–800.

4 M. Etxeberria–Benavides, T. Johnson, S. Cao, B. Zornoza, J. Coronas, J. Sanchez–Lainez, A. Sabetghadam, X. Liu, E. Andres–Garcia, F. Kapteijn, J. Gascon and O. David, *Sep. Purif. Technol.*, 2020, **237**, 116347.

5 M. Shan, X. Liu, X. Wang, Z. Liu, H. Iziyi, S. Ganapathy, J. Gascon and F. Kapteijn, *J. Mater. Chem. A*, 2019, **7**, 8929–8937.

6 M. Shan, X. Liu, X. Wang, I. Yarulina, B. Seoane, F. Kapteijn and J. Gascon, *Sci. Adv.*, 2018, **4**, eaau1698.

7 J. Sánchez–Laínez, M. Etxeberria–Benavides, O. David, C. Téllez and J. Coronas, *ChemSusChem*, 2021, **14**, 952–960.

8 A. Naderi, T.–S. Chung, M. Weber and C. Maletzko, *J. Membr. Sci.*, 2019, **591**, 117292.

9 S. Cong, Y. Yuan, J. Wang, Z. Wang and X. Liu, *AIChE J.*, 2023, **69**, e17983.

10 S. S. Hosseini, N. Peng and T. S. Chung, *J. Membr. Sci.*, 2010, **349**, 156–166.

11 V. M. Aceituno Melgar, H. T. Kwon and J. Kim, *J. Membr. Sci.*, 2014, **459**, 190–196.

12 L. Ma, F. Svec, T. Tan and Y. Lv, *J. Membr. Sci*., 2019, **576**, 1–8.

13 W. Li, Z. Yang, G. Zhang, Z. Fan, Q. Meng, C. Shen and C. Gao, *J. Mater. Chem. A*, 2014, **2**, 2110–2118.

14 W. Li, Q. Meng, C. Zhang and G. Zhang, *Chem. Eur. J*., 2015, **21**, 7224–7230.

15 X. Ma, Z. Wan, Y. Li, X. He, J. Caro and A. Huang, *Angew. Chem., Int. Ed.*, 2020, **59**, 20858–20862.

16 J. Liu, C. Liu and A. Huang, *Int. J. Hydrogen Energy*, 2020, **45**, 703–711.

17 P. Nian, Y. Li, X. Zhang, Y. Cao, H. Liu and X. Zhang, *ACS Appl. Mater. Interfaces*, 2018, **10**, 4151–4160.

18 S. Friebe, B. Geppert, F. Steinbach and J. Caro, *ACS Appl. Mater. Interfaces*, 2017, **9**, 12878–12885.

19 Y. Sun, C. Song, X. Guo and Y. Liu, *ACS Appl. Mater. Interfaces*, 2020, **12**, 4494–4500.

20 J. Lv, X. Zhou, J. Yang, L. Wang, J. Lu, G. He and Y. Dong, *J. Membr. Sci.*, 2022, **658**, 120585.

21 J. Hou, X. Hong, S. Zhou, Y. Wei and H. Wang, *AIChE J.*, 2019, **65**, 712–722.

22 J. Sánchez–Laínez, B. Zornoza, C. Téllez and J. Coronas, *J. Membr. Sci.*, 2018, **563**, 427–434.

23 H. Chang, Y. Wang, L. Xiang, D. Liu, C. Wang and Y. Pan, *Chem. Eng. Sci.*, 2018, 192, 85–93.

24 Q. Wang, Y. Tang, L. Liu, C. Liu, K. Zhang, X. Tian, X. Feng, R. Zhang, Y. Yu, T. Gu, B. Liu and S. Wang, *J. Membr. Sci.*, 2025, **726**, 124067.